COAGULATION

Synthetic oligosaccharides can replace animal-sourced low–molecular weight heparins

Yongmei Xu,[1] Kasemsiri Chandarajoti,[2,3] Xing Zhang,[4] Vijayakanth Pagadala,[1]* Wenfang Dou,[1] Debra Moorman Hoppensteadt,[5] Erica M. Sparkenbaugh,[2] Brian Cooley,[6] Sharon Daily,[7] Nigel S. Key,[2] Diana Severynse-Stevens,[7] Jawed Fareed,[5] Robert J. Linhardt,[4†] Rafal Pawlinski,[2†] Jian Liu[1†]

Low–molecular weight heparin (LMWH) is used clinically to treat clotting disorders. As an animal-sourced product, LMWH is a highly heterogeneous mixture, and its anticoagulant activity is not fully reversible by protamine. Furthermore, the reliability of the LMWH supply chain is a concern for regulatory agencies. We demonstrate the synthesis of heparin dodecasaccharides (12-mers) at the gram scale. In vitro experiments demonstrate that the anticoagulant activity of the 12-mers could be reversed using protamine. One of these, labeled as 12-mer-1, reduced the size of blood clots in the mouse model of deep vein thrombosis and attenuated circulating procoagulant markers in the mouse model of sickle cell disease. An ex vivo experiment demonstrates that the anticoagulant activity of 12-mer-1 could be reversed by protamine. 12-mer-1 was also examined in a nonhuman primate model to determine its pharmacodynamic parameters. A 7-day toxicity study in a rat model showed no toxic effects. The data suggest that a synthetic homogeneous oligosaccharide can replace animal-sourced LMWHs.

INTRODUCTION

Low–molecular weight heparins (LMWHs) are a widely prescribed class of anticoagulants used to prevent and treat arterial and venous thrombosis (*1*). LMWH is prepared through the chemical or enzymatic depolymerization of unfractionated porcine heparin (UFH) (*2*). Compared to UFH, LMWHs are more subcutaneously bioavailable, have a longer half-life, and show a decreased risk of heparin-induced thrombocytopenia (HIT), a life-threatening adverse effect associated with heparin (*3*, *4*). LMWHs can lower the risk of HIT by as much as 63%, substantially reducing HIT-related hospital expenditures (*5*). However, LMWHs cannot simply be substituted for standard unfractionated heparin in cases of HIT due to their cross-reactivity with HIT antibodies (*3*). Major hospitals and tertiary referral centers in the United States, Canada, and Europe are moving toward substituting LMWHs for UFH as prophylaxis for venous thromboembolism. The approval of generic forms of enoxaparin by the U.S. Food and Drug Administration (FDA) in 2010 has reduced the drug price, making LMWHs available to broader patient populations (*6*). LMWHs still have limitations. For example, LMWHs can be used in renal-impaired patients only at reduced doses (*7*), and their anticoagulant activity is only incompletely neutralized with protamine, thereby increasing bleeding risk. Although protamine can stop bleeding caused by enoxaparin in some patients, it is not generally viewed as a reliable method for neutralizing enoxaparin (*8*). Because LMWH is animal-sourced, the supply chain for LMWHs is under continued threat of contamination by adulterated products.

LMWH is a complex mixture of oligosaccharide natural products, consisting of a disaccharide repeating unit of either iduronic acid (IdoA) or glucuronic acid (GlcA) and glucosamine (GlcN) residues, with each residue capable of carrying sulfate groups. These oligosaccharides range from 6 to 30 residues long and display a wide range of sulfation patterns. Only a fraction of oligosaccharides in LMWH exhibit anticoagulant activity. The structural heterogeneity in LMWHs results in batch-to-batch differences in saccharide composition and sequence and anticoagulant activity (*6*).

Heparin is prepared from mucosa harvested from porcine intestine, requiring a long and poorly regulated supply chain. The quality and supply of LMWHs relies on the quality of animal-derived heparin. Batches of contaminated heparin that entered the worldwide market in late 2007 were responsible for many deaths, making this one of the worst incidents of a toxic drug product reaching the market in U.S. history (*9*). The contaminated heparin also adversely affected the purity of LMWHs (*10*), revealing the fragility of the LMWH supply chain. One form of synthetic heparin pentasaccharide, known as fondaparinux, is currently on the market (*11*). Fondaparinux is contraindicated for kidney-impaired patients, and its anticoagulant activity cannot be reversed by protamine (*12*). Thus, it is unlikely to substitute for enoxaparin.

We have been actively developing a method to prepare synthetic LMWH to bypass the need for animal-sourced heparin (*13*). Unlike traditional synthesis using a purely chemical approach, we rely on a chemoenzymatic synthesis method using a variety of heparin biosynthetic enzymes. Chemoenzymatic synthesis is a highly efficient method for preparing structurally heterogeneous heparin polysaccharides (*14*, *15*) as well as structurally homogeneous LMWH (*12*) and ultra-LMWH (*16*). This chemoenzymatic method also allows the design of LMWH oligosaccharide structures that display improved pharmacological properties. An LMWH synthesized by this method displays anticoagulant activity that is protamine-reversible, thereby reducing bleeding risk (*12*). However, until now, the chemoenzymatic synthesis could only be used to prepare a given product at the milligram scale and has been an impractical approach for the replacement of animal-sourced LMWHs.

[1]Division of Chemical Biology and Medicinal Chemistry, Eshelman School of Pharmacy, University of North Carolina, Chapel Hill, NC 27599, USA. [2]Division of Hematology/Oncology, Department of Medicine, University of North Carolina, Chapel Hill, NC 27599, USA. [3]Department of Pharmaceutical Chemistry, Faculty of Pharmaceutical Sciences, Prince of Songkla University, Hat Yai, Songkhla 90112, Thailand. [4]Department of Chemistry and Chemical Biology, Center for Biotechnology and Interdisciplinary Studies, Rensselaer Polytechnic Institute, Troy, NY 12180, USA. [5]Department of Pathology, Loyola University Medical Center, Maywood, IL 60660, USA. [6]Department of Pathology and Laboratory Medicine, School of Medicine, University of North Carolina, Chapel Hill, NC 27599, USA. [7]Center for Global Health, RTI International, Research Triangle Park, NC 27709, USA.
*Present address: Glycan Therapeutics LLC, Chapel Hill, NC 27599, USA.
†Corresponding author. Email: jian_liu@unc.edu (J.L.); rafal_pawlinski@med.unc.edu (R.P.); linhar@rpi.edu (R.J.L.)

Here, we report the design of a homogeneous LMWH oligosaccharide that is amenable to multigram-scale chemoenzymatic synthesis. The synthesized LMWH oligosaccharide was evaluated in disease-related mouse models, used for pharmacodynamic analysis in nonhuman primates, and examined by toxicological analysis in rats. The results suggest a cost-effective scheme for the preparation of a synthetic oligosaccharide as a substitution candidate for animal-sourced LMWHs.

RESULTS

Identification of synthetic LMWH constructs for scaled-up preparation

We synthesized two dodecasaccharides, 12-mer-1 and 12-mer-2 (Fig. 1A), using a chemoenzymatic method. The synthesis was initiated from a commercially available acceptor, *p*-nitrophenyl glucuronide (GlcA-pNP), using uridine diphosphate (UDP)–sugar donors, a glycosyltransferase, four or five different sulfotransferases, and an epimerase (Fig. 1B). The synthesis of 12-mer-1 was completed in 22 steps with an overall yield of 10.3%, and the synthesis of 12-mer-2 was completed in 23 steps with an overall yield of 8.2% (Fig. 1B and fig. S1). 12-mer-1 has one 3-*O*-sulfated glucosamine (GlcNS3S6S) residue that is located at residue C, whereas 12-mer-2 has two GlcNS3S6S residues that are located at residues C and G (Fig. 1A). These are different from our previously reported dodecasaccharide LMWH constructs (*12*), because their nonreducing end contains an *N*-sulfo glucosamine (GlcNS) residue in place of an *N*-acetyl glucosamine (GlcNAc) residue. This modification, suggested by analyzing the crystal structures of the 6-*O*-sulfotransferase (6-OST) (*17*), increased the reactivity of the substrate, making complete 6-*O*-sulfation considerably easier (reaction f, Fig. 1B). Six 6-*O*-sulfo groups were installed into each dodecasaccharide in a single reaction step. Complete 6-*O*-sulfation reaction avoided the necessity of purifying the product from a mixture of partial 6-*O*-sulfated 12-mers, increasing product purity and yield. A total of 1300 mg of 12-mer-1 and 110 mg of 12-mer-2 were synthesized (Fig. 1 and fig. S1).

Improvements in the enzyme and cofactor production also contributed to the success of our chemoenzymatic synthesis. Both C_5-epimerase (C_5-epi) and 2-*O*-sulfotransferase (2-OST) were expressed in insect cells using the baculovirus expression system (*18*). The activity levels of recombinant C_5-epi and 2-OST from insect cells were 225- and 75-fold greater, respectively, than the same enzymes expressed in *Escherichia coli*. The cost for Sf9 cell-conditioned medium was ~$60/liter, and the cost for *E. coli* culture was ~$3/liter. The excellent expression of C_5-epi and 2-OST offsets the higher costs of culturing insect cells. The syntheses

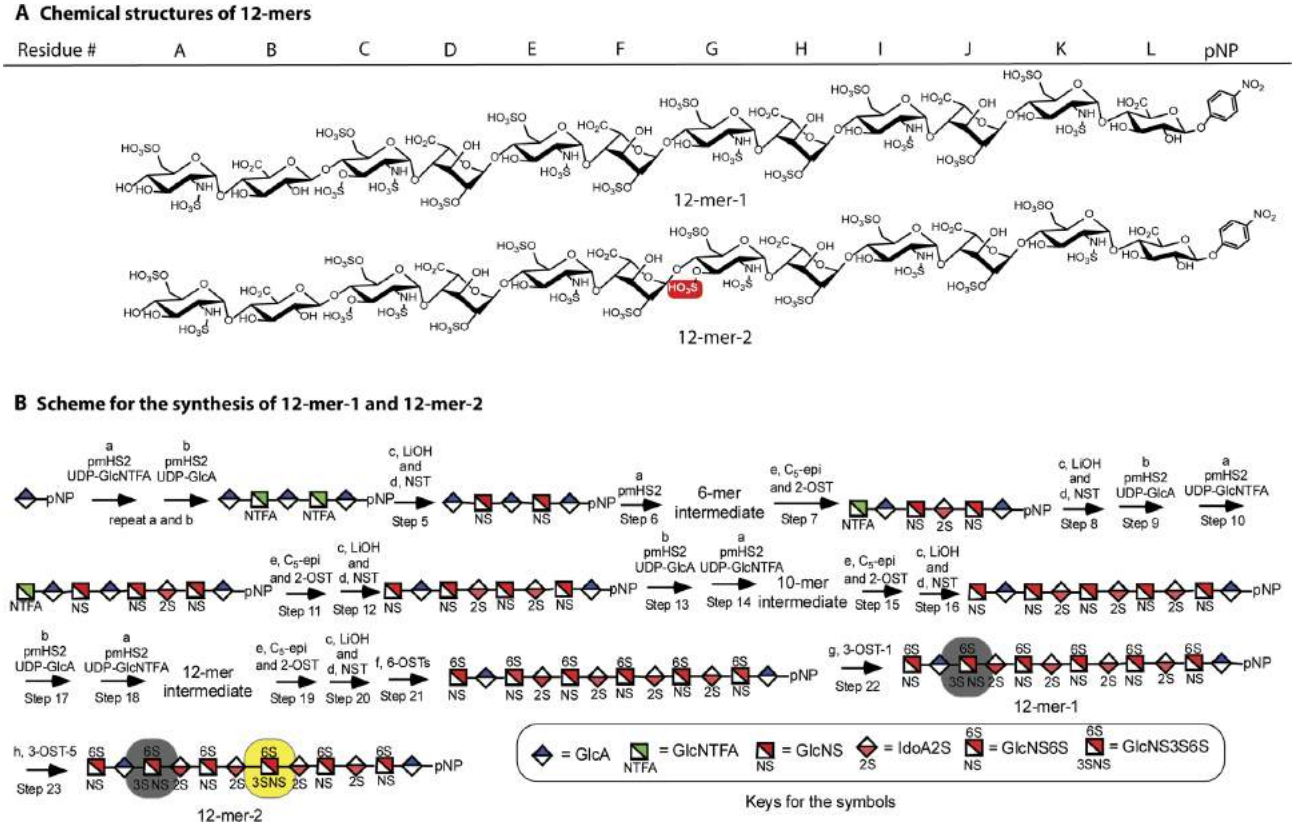

Fig. 1. Chemical structures and synthetic scheme of synthetic LMWHs, 12-mer-1 and 12-mer-2. (**A**) Chemical structures of 12-mer-1 and 12-mer-2. The name of each residue (A to L) is indicated at the top of the panel. The differences between two 12-mers are the number of 3-*O*-sulfo groups present: one in 12-mer-1 in residue C and two in 12-mer-2 in residues C and G (highlighted). pNP represents *p*-nitrophenyl group. (**B**) Synthetic schemes for 12-mer-1 and 12-mer-2 using shorthand symbols. Each reaction step uses different enzymes and chemicals: a, PmHS2 (heparosan synthase 2 from *Pasteurella multocida*) and UDP-GlcNTFA; b, PmHS2 and UDP-GlcA; c, LiOH; d, *N*-sulfotransferase (NST) and 3′-phosphoadenosine 5′-phosphosulfate (PAPS); e, C_5-epimerase (C_5-epi), 2-*O*-sulfotransferase (2-OST), and PAPS; f, 6-OST-1, 6-OST-3, and PAPS; g, 3-*O*-sulfotransferase isoform 1 (3-OST-1) and PAPS; h, 3-OST-5 and PAPS. Full synthetic schemes using chemical structures are shown in fig. S1.

of cofactors, including UDP-trifluoroacetyl glucosamine (GlcNTFA), UDP-GlcA, and PAPS, were accomplished using enzymes expressed in *E. coli* under a whole-cell format. This format permitted us to routinely carry out 20- to 50-g scale production to support the 12-mer syntheses, because it eliminated the required purifications of the enzymes used in cofactor synthesis.

The 12-mers were analyzed for purity by high-resolution anion-exchange high-performance liquid chromatography (HPLC). Structural analysis used high-resolution mass spectrometry (MS) and one-dimensional (1D) and 2D nuclear magnetic resonance (NMR) analyses. Both 12-mer-1 and 12-mer-2 showed a major single symmetric peak on the HPLC analysis, suggesting that the purities for both compounds were >98% (fig. S2). High-resolution MS analyses of 12-mer-1 and 12-mer-2 afforded observed masses of 3520.8280 and 3600.7848, respectively. These measured values were consistent with the calculated exact mass values of 3520.8928 (for 12-mer-1) and 3600.8550 (for 12-mer-2) (fig. S3). 1D and 2D NMR analyses confirmed the purity of 12-mer-1, and spectral assignment definitively provided its structure (figs. S4 to S8). Similar NMR analysis of 12-mer-2 confirmed its purity and provided many structural details (figs. S9 to S13), but the presence of its second 3-*O*-sulfo group required additional analyses. MS-based sequence analysis of 12-mer-2 was performed to precisely position its 3-*O*-sulfo groups (figs. S14 to S16) (*19*). Analysis of the products from 12-mer-2 formed by digestion with heparin lyases I and II allowed us to confirm the presence of a 3-*O*-sulfo group on residue G. A comparison of the NMR spectra of 12-mer-1 and 12-mer-2 (figs. S17 to S19) further supported their structural assignment.

In vitro and in vivo evaluation of the anticoagulant activities of the 12-mer oligosaccharides

The in vitro anticoagulant activity and its protamine neutralization were measured in comparison to UFH and to two other FDA-approved heparin drugs, fondaparinux and enoxaparin (Fig. 2, A to C). 12-mer-1 and 12-mer-2 displayed potent anti–factor Xa (FXa) activity with a median inhibitory concentration (IC_{50}) of 57 and 67 ng/ml, respectively (Fig. 2A). Similar IC_{50} values (21 and 35 ng/ml) for the anti-FXa activity were reported for two different 12-mers published previously (*12*). The anti–factor IIa (FIIa) activity of UFH was determined at the IC_{50} value of 86 ng/ml. However, neither 12-mer-1 nor 12-mer-2 displayed any inhibition of the activity of FIIa at the concentration of 50,000 ng/ml, making both oligosaccharides specific FXa inhibitors. The anti-FXa activities of 12-mer-1 and 12-mer-2 were reversible through the addition of protamine, and their sensitivity to protamine neutralization was comparable to that measured for UFH (Fig. 2B). Fondaparinux was completely insensitive to protamine neutralization, and the anti-FXa activity of enoxaparin was only partially neutralized using protamine (Fig. 2B). Subsequent biological studies focused on 12-mer-1 because it was easier to synthesize. In ex vivo experiments, administration of 12-mer-1 to a mouse also inhibited FXa activity, and its anti-FXa effect was diminished over 6 to 8 hours as the drug was cleared (fig. S20), confirming the anticoagulant activity of 12-mer-1.

Protamine neutralization of 12-mer-1 was also determined using an ex vivo mouse model. As a positive control for this model, the anti-FXa activity of UFH was effectively neutralized by protamine (Fig. 2C). Consistent with the results demonstrated in the in vitro analysis of

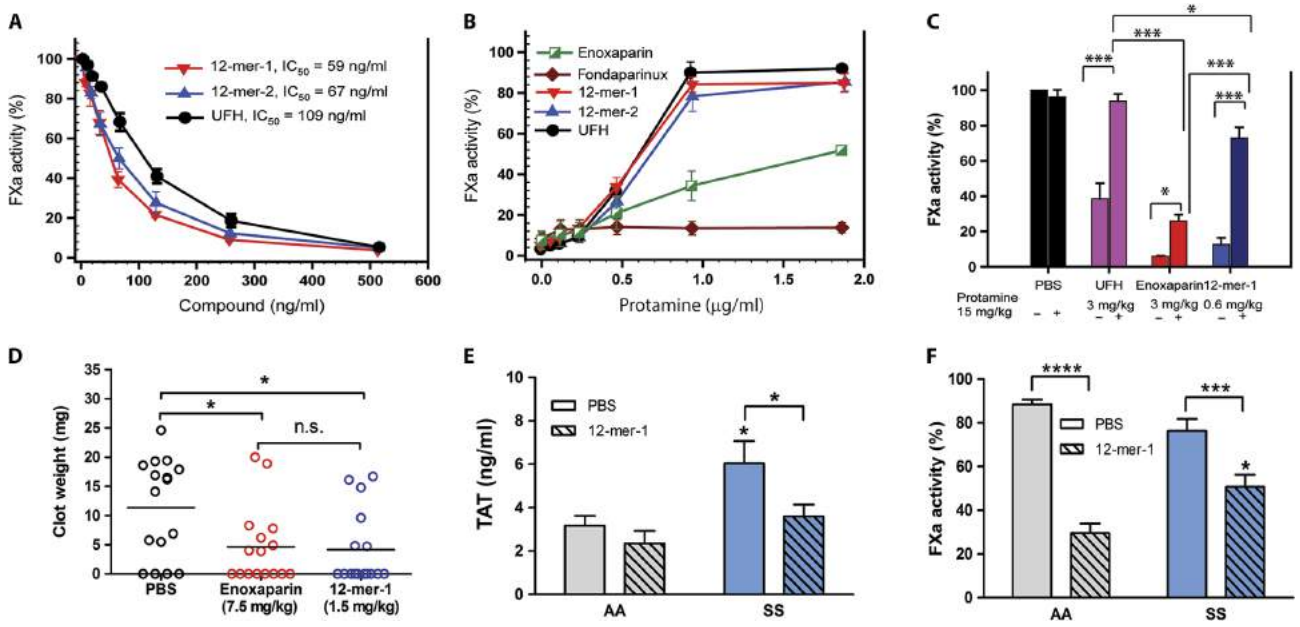

Fig. 2. In vitro, ex vivo, and in vivo analysis of the anticoagulant activity of 12-mers. (**A**) FXa inhibition curves of 12-mers and UFH in vitro. Data are means ± SD ($n = 4$). (**B**) Neutralization of FXa activity of 12-mers by protamine in vitro. In addition to 12-mers, UFH was included as a positive control, and fondaparinux and enoxaparin were included as negative controls. Data are means ± SD ($n = 4$). (**C**) Reversibility of anti-FXa activity by protamine in an ex vivo experiment. The statistical significance for the comparison of each sample with and without protamine is indicated ($P < 0.001$). (**D**) Reduction of clot weight in a venous thrombosis mouse model treated with PBS, enoxaparin, and 12-mer-1. (**E**) Plasma concentration of thrombin anti-thrombin (TAT) complexes and (**F**) FXa activity in control (AA) and sickle BERK (SS) mice injected with PBS or 12-mer-1 (2 mg/kg) subcutaneously every 8 hours for 7 days ($n = 8$ to 13). Blood was collected 2 hours after the last injection. Data are means ± SD. $^{*}P < 0.05$, $^{***}P < 0.001$, $^{****}P < 0.0001$. n.s., not significant.

12-mer-1, its anti-FXa activity was effectively reversed by protamine, whereas the activity of enoxaparin was only partially reversed (Fig. 2C). Protamine neutralization data indicate that the extent of FXa activity for UFH-treated mice was higher than that for 12-mer-1–treated mice, suggesting that some residual anti-FXa activity from 12-mer-1 still remained (Fig. 2C). The residual anti-FXa activity from 12-mer-1 could probably be neutralized using a higher concentration of protamine.

Evaluation of 12-mer-1 in disease models

A common indication for LMWH is for thromboprophylaxis in patients with a high risk of venous thromboembolism. Thus, we assessed the effect of 12-mer-1 on thrombosis in a mouse model of venous thrombosis induced by stenosis of the inferior vena cava (*20*, *21*). As expected, 24 hours after stenosis, 12-mer-1 significantly reduced clot weight (by ~60%, $P < 0.05$) compared to mice treated with phosphate-buffered saline (PBS) (Fig. 2D). Mice treated with enoxaparin showed a similar reduction of clot weight and incidence of thrombosis (Fig. 2D). These data demonstrate that 12-mer-1 reduces the formation of venous thrombosis. Notably, the dose of 12-mer-1 used in this experiment (1.5 mg/kg) was only one-fifth of the required dose of enoxaparin (7.5 mg/kg), showing that 12-mer-1 had considerably higher antithrombotic potency. One reason for this higher potency is that enoxaparin is composed of a mixture of active and inactive oligosaccharides, whereas 12-mer-1 is a homogeneous active oligosaccharide.

Next, we evaluated the anticoagulant properties of 12-mer-1 in a mouse model of sickle cell disease (SCD) (*22*). Chronic activation of coagulation is observed both in sickle cell patients and in the mouse model of the disease (*23*–*25*). SCD is also associated with multiple end-organ damage, including kidney (*26*, *27*). Sickle cell mice and control mice received subcutaneous injections of saline or 12-mer-1 (2.0 mg/kg) every 8 hours for 7 days. 12-mer-1 significantly attenuated the activation of coagulation in sickle cell mice ($P < 0.05$), as demonstrated by the reduction of plasma thrombin/antithrombin (TAT) complexes (Fig. 2E). At the end of the experiment, the FXa activity in the plasma of sickle cell mice was higher than in the plasma of control mice (Fig. 2F), suggesting that the accompanying kidney pathology in the sickle cell mice enhances, rather than reduces, the clearance of 12-mer-1. This result could be explained by the well-documented increase of renal blood flow and glomerular filtration rate observed in both sickle cell patients and mouse models of the disease (*28*, *29*).

Because LMWHs are cleared through the kidney, the dosing regimen must be reduced in renal-impaired patients. Therefore, we investigated the clearance of 12-mer-1 in mice with severe kidney failure caused by the removal of one kidney and by subjecting the remaining kidney to ischemia/reperfusion (I/R) injury (Fig. 3A). We confirmed that these experimental conditions caused acute kidney failure, demonstrated by increased plasma concentrations of creatinine at the end of the reperfusion period (2.19 ± 0.11 mg/dl versus 0.15 ± 0.03 mg/dl, respectively; $P < 0.0001$) in mice that had been operated on when compared to control mice undergoing a sham operation. UFH is considered to be safe for kidney-impaired patients (*30*), and thus, kidney failure does not alter the clearance of UFH, as demonstrated by similar FXa activity observed in the plasma of mice with kidney failure and control mice undergoing a sham operation (Fig. 3B). In contrast, compared to the sham-operated mice, the clearance of both high-dose (1.5 mg/kg) and low-dose (0.3 mg/kg) 12-mer-1 was significantly impaired in mice with kidney failure ($P < 0.05$), as demonstrated by a reduction of plasma FXa activity 2 hours after injection of 12-mer-1 (Fig. 3B). The impairment of 12-mer-1 clearance depends on the severity of the kidney injury. Reducing the severity of kidney injury by shortening the ischemic period increased plasma FXa activity in injured mice injected with 12-mer-1 at a dose of 0.3 mg/kg (Fig. 3C). These data demonstrate the impairment of 12-mer-1 clearance in mice suffering from kidney failure.

Pharmacodynamic analysis of 12-mer-1 in a nonhuman primate model

The 12-mer-1 oligosaccharide was administered to the *Macaca mulatta* primate model either intravenously or subcutaneously at a dose of 250 μg/kg. The plasma concentration of 12-mer-1 over time after administration was assessed by anti-FXa assay (fig. S21). On intravenous administration, the drug immediately distributed through the circulatory system. The earliest data point that was captured was 30 min after the

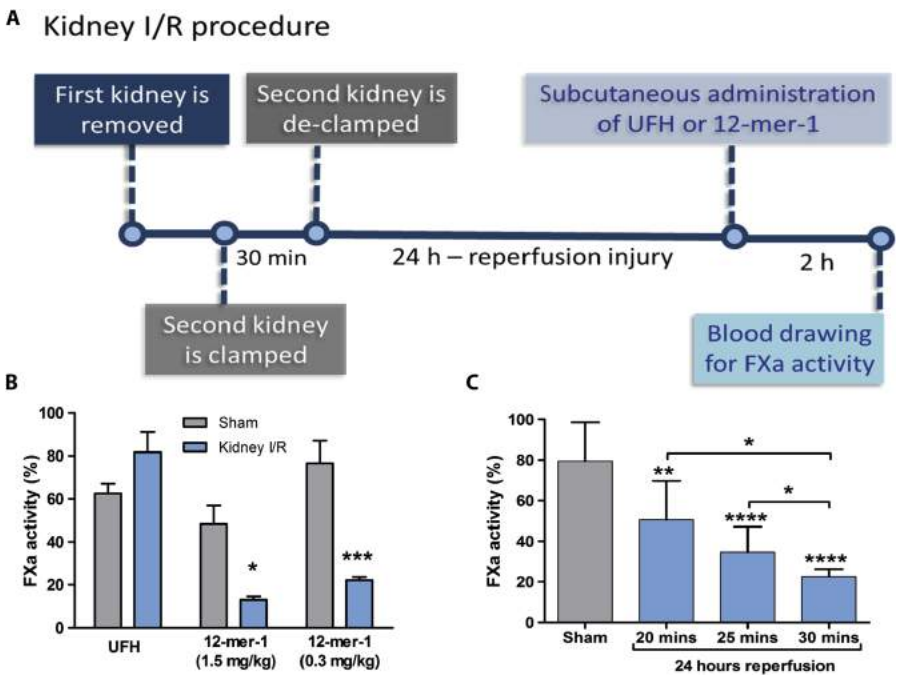

Fig. 3. Clearance of 12-mer-1 in kidney I/R injury model in C57BL/6J mice. (**A**) Kidney I/R experimental scheme. (**B**) Plasma activity of FXa in mice subjected to kidney I/R injury (30 min of ischemia time followed by 24 hours of reperfusion) and injected subcutaneously with UFH ($n = 6$; 3 mg/kg), 12-mer-1 ($n = 6$; 1.5 mg/kg), or 12-mer-2 ($n = 6$; 0.3 mg/kg). (**C**) Plasma activity of FXa in sham-operated mice and mice subjected to different ischemia periods (20, 25, and 30 min). Mice received subcutaneous injection of PBS or 12-mer-1 (0.3 mg/kg) after 24 hours of reperfusion, and plasma was collected 2 hours later ($n = 6$ for each group). $^{*}P < 0.05$, $^{**}P < 0.01$, $^{***}P < 0.001$, $^{****}P < 0.0001$.

injection (Fig. 4A). From the drug elimination profile, the calculated half-life of 12-mer-1 was 67 min. On subcutaneous administration, the drug reached a maximum plasma concentration 2 hours after injection (Fig. 4B). The calculated half-life for 12-mers administered through the subcutaneous route was 2.9 hours. A higher dose of 12-mer-1 (500 μg/kg) was next administered by intravenous and subcutaneous routes (fig. S22). At this higher dose, the half-lives for intravenous and subcutaneous routes were 72 min and 3.4 hours, respectively. The data demonstrate that whereas the route of administration affects the clearance rate, the dose does not.

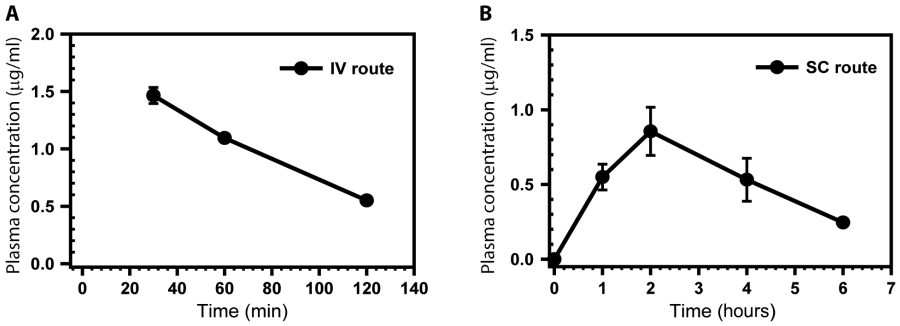

Fig. 4. Clearance of 12-mer-1 from a nonhuman primate model. *M. mulatta* monkeys were treated with 12-mer-1 at a dose of 250 μg/kg either intravenously (IV) (**A**) or subcutaneously (SC) (**B**). Blood samples were collected before dosing (at $t = 0$ hour) and at 30, 60, and 120 min after dosing (for IV group) or at 1, 2, 4, and 6 hours after dosing (for SC group). The plasma concentration of 12-mer-1 was determined by measuring the activity of FXa, which was converted into the concentration of 12-mer-1 by a standard curve, as shown in fig. S21. Data are average ± range ($n = 2$).

Toxicology studies of 12-mer-1

Toxicology studies on 12-mer-1 were performed in Sprague-Dawley rats. Here, a single dose of 3600 μg/kg per day, 7.2- to 14.4-fold higher than the dose used in the nonhuman primate model, was intravenously given to rats for seven consecutive days. Blood samples were drawn for serum chemistry analysis at day 8, and all organs were harvested to measure the organ and body weights (Table 1). All serum chemistry parameters in the 12-mer-1–treated animals were essentially identical to those from the control group. A decrease in total white blood cells was observed in the treated group; however, these values were within the laboratory's historical control data range and, thus,

Table 1. Toxicological results and organ weights.

Parameters	Control ($n = 5$)	3600 μg/kg ($n = 5$)	Historical control values*
White blood cells ($\times 10^3/\mu l$)	9.9 ± 1.1	7.8 ± 1.0	9.6 ± 3.0
Red blood cells ($\times 10^6/\mu l$)	8.3 ± 0.2	8.1 ± 0.3	8.5 ± 0.6
Hemoglobin (g/dl)	15.1 ± 0.4	14.8 ± 0.3	15.9 ± 0.9
Blood urea nitrogen (mg/dl)	18.0 ± 2.2	17.8 ± 2.4	18 ± 3.2
Creatinine (mg/dl)	0.40 ± 0.01	0.42 ± 0.03	0.46 ± 0.12
Albumin (g/dl)	3.54 ± 0.06	3.62 ± 0.08	3.4 ± 0.17
Total bilirubin (mg/dl)	0.11 ± 0.01	0.10 ± 0.01	0.12 ± 0.024
Alanine aminotransferase (U/liter)	43.6 ± 8.1	38.6 ± 2.4	46 ± 15.3
Total protein (g/dl)	6.18 ± 0.16	6.28 ± 0.11	6.2 ± 0.41
Body weight (g)†	268.4 ± 4.2	271.4 ± 5.9	
Organ–to–body weight ratio†			
Brain	0.69 ± 0.04	0.71 ± 0.02	
Adrenal glands	0.026 ± 0.014	0.020 ± 0.004	
Heart	0.41 ± 0.04	0.41 ± 0.02	
Kidneys	0.73 ± 0.05	0.70 ± 0.04	
Liver	3.04 ± 0.09	3.04 ± 0.11	
Spleen	0.25 ± 0.01	0.25 ± 0.02	
Testes	1.36 ± 0.04	1.29 ± 0.06	
Thyroid/parathyroid	0.0062 ± 0.0011	0.0058 ± 0.0011	

*The historical control value was obtained from the analysis of ~1750 individual normal rats. †Body weight and organ weight were measured on day 8.

are not considered toxicologically adverse. The organ–to–body weight ratios among treated and control groups were indistinguishable. Two additional dose regimens for 12-mer-1, 400 and 1200 μg/kg per day, were also examined in these studies (table S1). Together, the data confirm that 12-mer-1 is well tolerated, dampening concern about the potential toxicity of the *p*-nitrophenyl group present at the reducing end of 12-mer-1 (*12*, *31*).

DISCUSSION

The introduction of LMWHs in the 1990s afforded a relatively safe class of subcutaneously bioavailable anticoagulant drugs. LMWHs remain as the drug class of choice for cancer patients (*32*) and pregnant women (*33*) despite the emergence of newer nonheparin oral anticoagulant drugs in recent years. However, the reliance on a single animal species coming predominately from one country for the LMWH supply chain and the burden imposed on regulatory agencies for ensuring the safety of structurally heterogeneous LMWH products remain serious concerns. Despite extensive efforts from the FDA and U.S. Pharmacopeia to improve the purity analysis after the heparin crisis in 2007, the animal-sourced heparin is still not 100% risk-free because of the lack of "unequivocal and specific analytical techniques" (*9*). The U.S. Congressional Committee on Energy and Commerce has also raised concerns over the safety of the heparin supply chain in a letter to the FDA in 2016 (https://energycommerce.house.gov/news-center/press-releases/committee-leaders-express-continued-concern-fda-s-califf-about). These actions from the regulatory agency and the U.S. Congress demonstrate that the safety of the supply of heparin and LMWH is of interest.

A major challenge for the penetration of the heparin market by homogeneous heparin products is the ability to cost-effectively synthesize such compounds. There are concerns over the scalability of chemoenzymatic synthesis of LMWH. Here, we report the gram-scale synthesis of a homogeneous dodecasaccharide and demonstrate it to be a candidate to replace LMWHs in thromboprophylaxis. Our synthesis was accomplished using standard equipment found in an academic laboratory by carefully designing the structure of the target oligosaccharide, improving the expression of heparin biosynthetic enzymes and cofactor production. The scale of the synthesis can be increased in a pilot plant or an industrial facility with large-scale fermentation and liquid-handling equipment. There is no doubt that substantial optimization and improvement for the processes of the expression of enzymes and product purification will be required to be suitable for industrial-scale synthesis. One notable successful example that translates a laboratory synthesis to industrial production is the synthesis of fondaparinux, which involves ~50 synthetic steps. The first synthesis was only completed at the milligram scale (*34*, *35*), but it is now synthesized at the kilogram scale (*36*). The product occupies a sizeable share of heparin market.

Enoxaparin has a half-life of 5 to 6 hours when subcutaneously administered in the same nonhuman primate model used in the current study (*37*). Similar elimination rates observed for 12-mer-1 and enoxaparin offer an insight for designing the dose regimen for future human clinical trials. Enoxaparin is administered either twice a day or once a day as thromboprophylaxis in the clinic. We anticipate that 12-mer-1 could be used in a similar regimen, although at lower doses than enoxaparin, because 12-mer-1 is a more potent compound.

Previously, we reported that dodecasaccharides with similar structures bound to stabilin-2 receptors on the liver sinusoidal endothelium, suggesting that a ^{35}S-labeled dodecasaccharide at a low dose is cleared by the liver rather than kidney (*12*). The current study found that the clearance of 12-mer-1 is impaired in the mice with I/R-injured kidneys, a model for kidney failure. These data suggest that 12-mer-1 may accumulate in patients with severe kidney impairment, increasing the risk for bleeding. Fortunately, because 12-mer-1 is a structurally homogeneous compound, it would allow a dose adjustment for kidney failure patients.

In contrast to the reduced clearance observed in mice with severe kidney failure, clearance of 12-mer-1 was modestly increased in SCD mice. This is likely due to an increased renal blood flow and glomerular filtration rate described in children and young adults with SCD as well as sickle cell mice (*28*, *29*). Renal hyperfiltration in SCD increases proximal tubular transport, which is the dominant mechanism responsible for renal excretion of LMWH (*38*) and, most likely, excretion of 12-mer-1. Renal filtration in SCD normalizes with age or after the development of nephropathy and is reduced below normal as nephropathy progresses into overt renal failure.

The overall risk of major bleeding associated with LMWH is 1 to 4% (*39*). The reversibility of 12-mer-1 anticoagulant activity using protamine should improve the safety of anticoagulant therapy. Protamine, a polycationic polypeptide, is used to neutralize UFH; however, adverse effects have been reported (*40*). Newer reversing agents have recently emerged (*41*, *42*). For instance, an engineered FXa-like protein, known as andexanet, neutralizes the effects of LMWH as well as oral direct FXa inhibitors such as rivaroxaban and apixaban (*42*). Results from clinical trials indicate that andexanet is well tolerated by patients and effectively reverses bleeding effects caused by rivaroxaban or apixaban with 81% (26 of 32 patients) and 65% (20 of 31 patients) efficacy, respectively (*43*, *44*). However, only one in four patients (25%) treated with enoxaparin responded effectively to andexanet treatment (*44*). One plausible explanation is that enoxaparin displays both anti-FXa and anti-FIIa activity, whereas andexanet is designed to be a specific agent for reversing FXa-specific inhibitors. If this is the case, then we anticipate that andexanet would be more effective in neutralizing the specific anti-FXa activity of 12-mer-1.

The introduction of heparin and LMWHs has advanced modern medicine, as demonstrated by their widespread application in surgical procedures and in kidney dialysis. A cost-effective method to prepare synthetic LMWH should improve the safety and reliability of these life-saving drugs. The next generation of safer, reliable, and affordable synthetic LMWH drugs should greatly benefit patients.

MATERIALS AND METHODS

Study design

This study was designed to synthesize homogeneous 12-mers with the goal of replacing animal-sourced LMWHs. We demonstrate the chemoenzymatic synthesis of two 12-mers that can substitute for LMWHs. The synthesis of 12-mers was repeated more than two times. The structures were confirmed using both NMR and high-resolution MS. Biological evaluation was conducted to evaluate the anticoagulant activity of the synthesized 12-mers. FXa activity was used as a surrogate to assess the anticoagulant activity. The reversal effect of protamine on the anticoagulant activity of 12-mers was also assessed by FXa assay. The in vitro anti-FXa activity measurement and protamine reversibility experiment were repeated three times. The murine studies were performed with blinding; the rat and nonhuman primate studies were not blinded. Animals were randomly assigned to the control or treated groups. The number of animals in each experiment was determined on the basis of previous experiences. The in vivo anti-FXa activity and protamine

reversibility effect were performed in mice with four animals in each group, and no outliers were found. A mouse model of venous thrombosis induced by stenosis of the inferior vena cava was used to determine the antithrombotic effects of 12-mer-1 with eight animals in each cohort. This experiment was repeated twice. The pharmacodynamic study in monkeys was completed in two doses with two animals per group. A 7-day toxicity study was completed in a rat model with five rats in each cohort. A total of three doses were administered to rats to determine toxic effects, but none were observed. A detailed description of Materials and Methods is provided below and is included in the Supplementary Materials.

Chemoenzymatic synthesis of 12-mers

The synthesis of 12-mer-1 and 12-mer-2 was completed according to the chemoenzymatic method published previously (*12*, *45*). Briefly, PmHS2 from *P. multocida* was used in conjunction with UDP-sugars to elongate the monosaccharide, GlcA-pNP, to appropriate-sized backbones. The backbone was then subjected to modification with NST, C_5-epi, 2-OST, 6-OST, 3-OST-1, and 3-OST-5. There were seven major steps involved in the overall synthesis, including step a (elongation step to add GlcNTFA), step b (elongation step to add GlcA), step c (detrifluoroacetylation), step d (*N*-sulfation step), step e (2-*O*-sulfation/epimerization), step f (6-*O*-sulfation step), step g (3-*O*-sulfation by 3-OST-1), and step h (3-*O*-sulfation by 3-OST-5) (Fig. 1B and fig. S1). These steps were repeated to prepare the final 12-mer products. The products were purified by anion-exchange chromatography using a Q Sepharose column. The structures of the products were proven by NMR and high-resolution MS.

Removal of endotoxin from 12-mer-1

12-mer-1 (450 mg) was dissolved in 4 ml of endotoxin-free water and then filtered through a 50-ml centrifugal filter unit (Amicon Ultra-15, Ultracel-100k; Merck Millipore) at 4000 rpm for 10 min. The process was repeated four times by refilling the sample chamber with 3 ml of water each time. The filtered solution was collected and dried. The level of endotoxin was measured using the Limulus Amebocyte Lysate (LAL) Kit (Associates of Cape Cod Inc.). Briefly, the LAL test was performed by adding 0.1 ml of reconstituted Pyrotell (sensitivity, 0.03 endotoxin units/ml) to 0.1 ml of the test sample, 12-mer-1, at various concentrations (96, 48, 24,12, 6, 3, and 1.5 μg/ml) in a 10 mm × 75 mm depyrogenated glass reaction tube (Associates of Cape Cod Inc.). The reaction solution was mixed thoroughly and placed immediately in a dry block incubator at 37°C for 60 ± 2 min. At the end of the incubation, the tube was removed and inverted 180°. If a gel clot was formed and remained intact in the bottom of the tube, the test was considered positive for endotoxin presence, and the concentration of endotoxin was determined to be greater than or equal to the sensitivity of Pyrotell.

Determination of the in vitro and ex vivo anti-FXa and anti-FIIa activity

Assays were based on a previously published method (*46*, *47*). Briefly, human FXa (Enzyme Research Laboratories) was diluted to 50 U/ml with PBS. The chromogenic substrate S-2765 (Diapharma) was diluted to 1 mg/ml in water. UFH (U.S. Pharmacopeia), enoxaparin (from local pharmacy), fondaparinux, and 12-mers were dissolved in PBS at various concentrations (3 to 600 μg/ml). The reaction mixture, which consisted of 20 μl of human plasma (Sigma-Aldrich) and 45 μl of the solution containing the sample at different concentrations, was incubated at room temperature for 5 min. FXa (100 μl) was then added. After incubating the reaction at room temperature for 4 min, we added 30 μl of the S-2765 substrate. The absorbance of the reaction mixture was measured at 405 nm continuously for 5 min. The absorbance values were plotted against the reaction time. The initial reaction rates as a function of concentration were used to calculate the IC_{50} values.

Anti-FIIa activity assays were based on a previously published method (*48*). Briefly, thrombin from bovine plasma (Sigma-Aldrich) was diluted to 10 U/ml in PBS with bovine serum albumin (1 mg/ml). The chromogenic substrate S-2238 (Diapharma) was made up at 1 mg/ml in PBS. UFH (U.S. Pharmacopeia) and 12-mers were dissolved in PBS at various concentrations (0.1 to 5 ng/μl and 10 ng/μl to 1 μg/μl). The reaction mixture, which consisted of 60 μl of antithrombin (35 μg/ml, Cutter Biologics) and 10 μl of the solution containing the sample, was incubated at room temperature for 2 min. Thrombin (100 μl) was then added. After incubating at room temperature for 4 min, 30 μl of the S-2238 substrate was added. The absorbance of the reaction mixture was measured at 405 nm continuously for 5 min. The absorbance values were plotted against the reaction time. The initial reaction rates as a function of concentration were used to calculate the IC_{50} values.

Neutralization of synthetic 12-mers by protamine

The procedures followed a previous publication (*49*). The 12-mers and protamine chloride (Sigma-Aldrich) were dissolved in PBS. The concentrations of the 12-mers were different because each construct has a different IC_{50} value for the anti-FXa activity. The reaction mixture consisted of 20 μl of human plasma (Sigma-Aldrich); 45 μl of the stock solutions of enoxaparin, UFH, fondaparinux, and 12-mers (the concentration was 25 × IC_{50}); and 20 μl of protamine at various concentrations (from 0 to 90 μg/ml), and was incubated at room temperature for 5 min. The mixture (85 μl) was then subjected to anti-FXa activity measurement as described above.

Neutralization of 12-mer-1 by protamine in mice

The study was performed on 8-week-old male C57BL/6J mice (The Jackson Laboratory) (n = 4 per group). The mouse experiments were approved by the University of North Carolina (UNC) Animal Care and Use Committees and complied with National Institutes of Health guidelines. Under isoflurane anesthesia, mice were subcutaneously treated with PBS, UFH (3 mg/kg), enoxaparin (3 mg/kg), or 12-mer-1 (0.6 mg/kg) 30 min before protamine administration. Protamine (15 mg/kg) or PBS was administered intravenously through retro-orbital plexus injection, and 5 min later, blood samples were drawn from the inferior vena cava into syringes preloaded with 3.2% solution of sodium citrate (blood/citrate solution ratio was 9:1). To obtain mouse plasma, blood samples were centrifuged at 4000*g* for 15 min at 4°C. Mouse plasma was then used to determine anti-FXa activity. Ex vivo analysis of anti-FXa activity was done similar to the in vitro study described above. The anti-FXa activity in the mouse plasma from the PBS-injected mice was defined as 100%. Statistical analysis for multiple comparisons was performed by two-way analysis of variance (ANOVA) with Bonferroni's post hoc test (GraphPad Prism Software).

Evaluation of in vivo thrombosis in a murine vena cava stenosis model

A murine model of thrombosis (also known as St. Thomas Model) (*20*) was used to evaluate the anticoagulant potential of the 12-mers. Briefly, adult male Balb/c mice (The Jackson Laboratory) were anesthetized with an intraperitoneal ketamine (100 mg/kg)/xylazine (15 mg/kg) cocktail, and the infrarenal vena cava was exposed. Major side branches were ligated with 5-0 silk. A stenosis was created in the vena cava just

caudal to the left renal vein by using a 5-0 nylon spacer, placing a 5-0 ligature around both the vena cava and the spacer, and then removing the spacer after tying the ligature. A mini bulldog clamp (#18053-28, Fine Science Tools) was then applied for 15 s onto the vena cava caudal to the ligation point at two different locations. The wound was closed in two layers. Subcutaneous injections of the 12-mers (1.5 mg/kg), enoxaparin (7.5 mg/kg), or PBS control were given at 30 min, 5 hours, and 10 hours after the creation of the stenosis. Mice were reanesthetized at 24 hours, and the clots were harvested and weighed. Statistical analysis for multiple comparisons was performed by one-way ANOVA with Bonferroni's post hoc test (GraphPad Prism Software).

Mouse model of SCD

BERK mice on a mixed genetic background (FVB/N, 129, DBA/2, C57BL/6, and Black Swiss) were used (*22*). BERK mice have a transgene containing normal human α-, γ-, δ-globins; sickle β-globin; and targeted deletions of murine α- and β-globins ($\alpha^{-/-}$, $\beta^{-/-}$, Tg). We generated these mice by intercrossing $\alpha^{-/-}$, $\beta^{-/-}$, Tg males with $\alpha^{-/-}$, $\beta^{+/-}$, Tg females. As a control, we used wild-type (WT) mice on a similar mixed genetic background that have no human transgenes ($\alpha^{+/+}$, $\beta^{+/+}$). Four- to 6-month-old mice were used. All mouse experiments were approved by the UNC Animal Care and Use Committees and complied with National Institutes of Health guidelines.

The anticoagulant effect of 12-mer-1 in SCD model

Four-month-old BERK and WT mice (both male and female) received subcutaneous injection of PBS or 12-mer-1 (2 mg/kg) every 8 hours for 7 days. Blood was collected from the inferior vena cava 2 hours after the last injection to quantify plasma FXa activity and TAT.

Determination of TAT

Mouse plasma concentration of TAT was analyzed using commercial enzyme-linked immunosorbent assay following the manufacturer's instructions (Siemens Healthcare Diagnostics).

Mouse model of kidney failure induced by I/R injury

Severe kidney failure was induced in 2- to 3-month-old C57BL/6 male mice (The Jackson Laboratory) by subjecting them to a unilateral I/R with simultaneous contralateral nephrectomy (*50*). Briefly, mice were anesthetized with a mixture of ketamine (80 mg/kg)/xylazine (16 mg/kg). Mice underwent a midline laparotomy followed by the removal of one kidney. Unilateral ischemia was induced by clamping the renal artery on the other kidney at the desired ischemia time using a vascular clip. At the end of ischemia, the clip was removed and kidney reperfusion was visually confirmed as return of blush color, after which the abdomen was closed with sutures. Sham-operated mice were only subjected to laparotomy. After 24 hours of reperfusion, mice were subjected to subcutaneous administration of PBS or anticoagulant agents. Two hours after treatment, blood was collected from the inferior vena cava into 3.8% solution of sodium citrate (9:1, v/v). All mouse experiments were approved by the UNC Animal Care and Use Committees and complied with National Institutes of Health guidelines.

The anticoagulant effect of 12-mer-1 in kidney I/R injury model

In one study, mice with contralateral nephrectomy were subjected to 30 min of ischemia on the other kidney. After 24 hours of kidney reperfusion, mice were subcutaneously treated with UFH ($n = 6$, 3 mg/kg) and two different doses of 12-mer-1: 1.5 mg/kg ($n = 6$) and 0.3 mg/kg ($n = 6$). Two hours after treatment, blood was collected to obtain mouse plasma to determine FXa activity. In another study, mice with contralateral nephrectomy were subjected to various ischemia times (20, 25, and 30 min) on the other kidney to modulate the severity of the kidney injury. After 24 hours of kidney reperfusion, mice were subcutaneously treated with 12-mer-2 (0.3 mg/kg; $n = 6$ for each group). Two hours after injection, blood was collected to obtain mouse plasma to determine FXa activity.

Pharmacodynamic analysis in nonhuman primates

The detailed procedures were described previously (*37*). Briefly, nonhuman primates (*M. mulatta*) were anesthetized with an intramuscular injection of ketamine (Ketaset, Fort Dodge Animal Health) and xylazine (AnaSed injection, Lloyd Laboratories). Upon anesthesia, the primates were weighed and a baseline blood sample was collected by saphenous vein puncture. A site on the abdomen was shaved and cleansed by alternate wiping with betadine and ethanol before subcutaneous administration of endotoxin-free 12-mer-1 at a dose of 250 or 500 μg/kg using a tuberculin syringe attached to a 21-gauge needle. Intravenous administration of 12-mer-1 at a dose of 250 or 500 μg/kg using a butterfly (21-gauge) needle placed in the contralateral saphenous vein was also performed. For both the subcutaneous and intravenous studies, working concentrations of 2.5 and 5 mg/ml were made in sterile saline. Blood samples were collected at 1, 2, 4, and 6 hours after subcutaneous administration or at 0.5, 1, and 2 hours after intravenous administration. All blood samples were centrifuged within 15 min of collection to make platelet-poor plasma. The plasma was stored at −70°C until analysis. Plasma samples were subjected to anti-FXa activity analysis using the chromogenic substrate method.

Toxicology studies

The studies were carried out by Calvert Labs following standard protocols for acute toxicity testing (*51*). Endotoxin-free 12-mer-1 (400 mg) was prepared as dosing solutions in 0.9% NaCl for injection (saline solution). Experimentally naïve Sprague-Dawley male rats were about 9 to 11 weeks old at the start of dosing phase. The animals' weight range at the start of the repeat-dose phase was 249 to 274 g. Separate groups of five male rats were given 12-mer-1 at dose levels of 0, 400, 1200, and 3600 μg/kg per dose by intravenous bolus injection via the lateral tail vein for seven consecutive days. Rats were observed daily for clinical signs before dosing and 1 to 2 hours after dose administration. Animals were observed for clinical signs until scheduled necropsy on day 8. There were no early deaths and no adverse effects with the exception of red staining around the left eye on days 2 and 3 for one male in the 1200 μg/kg per dose group. No clinical signs of toxicity were observed over the 7-day dosing period in any animal.

Body weights were recorded before drug administration on days 1, 4, and 7. Food consumption was recorded on days 1 and 7 to calculate food consumption for the dosing period. On day 8, five rats per group were euthanized by CO_2 asphyxiation. At scheduled necropsy, whole-blood samples were collected for evaluation of specific hematology and serum chemistry parameters. Gross pathologic findings were recorded, selected organs were weighed, and selected tissues were harvested and preserved. No abnormalities were observed during the course of the study.

Statistical analysis

All statistical analyses were performed using GraphPad Prism (version 5.0). Data are represented as means ± SD unless specifically indicated in

the text. For two-group comparison of continuous data, a two-tailed Student's *t* test was used. For multiple-group comparison, data were analyzed by one- or two-way ANOVA followed by Bonferroni multiple comparisons. $P \leq 0.05$ was regarded as significant.

SUPPLEMENTARY MATERIALS

www.sciencetranslationalmedicine.org/cgi/content/full/9/406/eaan5954/DC1
Materials and Methods
Fig. S1. Chemoenzymatic synthetic scheme for 12-mer-1 and 12-mer-2.
Fig. S2. Anion exchange HPLC chromatograms of 12-mer-1 and 12-mer-2.
Fig. S3. High-resolution MS analysis of 12-mer-1 and 12-mer-2 by HILIC-FT MS.
Fig. S4. ^{1}H and ^{13}C NMR spectra of 12-mer-1.
Fig. S5. ^{1}H-^{1}H COSY and ^{1}H-^{13}C HSQC NMR spectra of 12-mer-1.
Fig. S6. ^{1}H-^{1}H NOESY and ^{1}H-^{1}H TOCSY NMR spectra of 12-mer-1.
Fig. S7. ^{1}H-^{13}C HMBC spectrum of 12-mer-1.
Fig. S8. ^{1}H NMR/^{13}C NMR chemical shift assignments (in ppm) of 12-mer-1.
Fig. S9. ^{1}H and ^{13}C NMR spectra of 12-mer-2.
Fig. S10. ^{1}H-^{1}H COSY and ^{1}H-^{13}C HSQC spectra of 12-mer-2.
Fig. S11. ^{1}H-^{1}H NOESY and ^{1}H-^{1}H TOCSY spectra of 12-mer-2.
Fig. S12. ^{1}H-^{13}C HMBC spectrum of 12-mer-2.
Fig. S13. ^{1}H NMR/^{13}C NMR chemical shift assignments (in ppm) of 12-mer-2.
Fig. S14. Determining the structure of 12-mer-2 by heparin lyase II digestion.
Fig. S15. Determination of the 3-*O*-sulfo group in 12-mer-2 by partial heparin lyase II digestion.
Fig. S16. Confirmation of the location of the 3-*O*-sulfo group in 12-mer-2 by partial heparin lyase I digestion.
Fig. S17. Comparison of 2D ^{1}H-^{1}H COSY with ^{1}H NMR.
Fig. S18. Comparison of 2D ^{1}H-^{13}C HSQC of 12-mer-1 and 12-mer-2.
Fig. S19. Comparison of 2D ^{1}H-^{1}H TOCSY and NOESY spectra of 12-mer-2.
Fig. S20. The effect of 12-mer-1 on the activity of FXa in mice.
Fig. S21. In vitro assay method and standard curve of 12-mer-1 for pharmacodynamic studies in nonhuman primates.
Fig. S22. Elimination profiles of 12-mer-1 in primate through intravenous or subcutaneous administration at 500 μg/kg.
Table S1. Additional toxicological data and organ and body weight ratios.
References (*52*–*57*)

REFERENCES AND NOTES

1. S. R. Kahn, W. Lim, A. S. Dunn, M. Cushman, F. Dentali, E. A. Akl, D. J. Cook, A. A. Balekian, R. C. Klein, H. Le, S. Schulman, M. H. Murad, Prevention of VTE in nonsurgical patients: Antithrombotic Therapy and Prevention of Thrombosis, 9th ed: American College of Chest Physicians Evidence-Based Clinical Practice Guidelines. *Chest* **141** (suppl. 2), e195S–e226S (2012).
2. R. J. Linhardt, J. Liu, Synthetic heparin. *Curr. Opin. Pharmacol.* **12**, 217–219 (2012).
3. A. Greinacher, Heparin-induced thrombocytopenia. *N. Engl. J. Med.* **373**, 252–261 (2015).
4. N. Martel, J. Lee, P. S. Wells, Risk for heparin-induced thrombocytopenia with unfractionated and low-molecular-weight heparin thromboprophylaxis: A meta-analysis. *Blood* **106**, 2710–2715 (2005).
5. K. E. McGowan, J. Makari, A. Diamantouros, C. Bucci, P. Rempel, R. Selby, W. Geerts, Reducing the hospital burden of heparin-induced thrombocytopenia: Impact of an avoid-heparin program. *Blood* **127**, 1954–1959 (2016).
6. S. Lee, A. Raw, L. Yu, R. Lionberger, N. Ya, D. Verthelyi, A. Rosenberg, S. Kozlowski, K. Webber, J. Woodcock, Scientific considerations in the review and approval of generic enoxaparin in the United States. *Nat. Biotechnol.* **31**, 220–226 (2013).
7. S. Harder, Renal profiles of anticoagulants. *J. Clin. Pharmacol.* **52**, 964–975 (2012).
8. J. E. Ansell, B. E. Laulicht, S. H. Bakhru, M. Hoffman, S. S. Steiner, J. C. Costin, Ciraparatag safely and completely reverses the anticoagulant effects of low molecular weight heparin. *Thromb. Res.* **146**, 113–118 (2016).
9. A. Y. Szajek, E. Chess, K. Johansen, G. Gratzl, E. Gray, D. Keire, R. J. Linhardt, J. Liu, T. Morris, B. Mulloy, M. Nasr, Z. Shriver, P. Torralba, C. Viskov, R. Williams, J. Woodcock, W. Workman, A. Al-Hakim, The US regulatory and pharmacopeia response to the global heparin contamination crisis. *Nat. Biotechnol.* **34**, 625–630 (2016).
10. Z. Zhang, M. Weïwer, B. Li, M. M. Kemp, T. H. Daman, R. J. Linhardt, Oversulfated chondroitin sulfate: Impact of a heparin impurity, associated with adverse clinical events, on low-molecular-weight heparin preparation. *J. Med. Chem.* **51**, 5498–5501 (2008).
11. M. Petitou, C. A. A. van Boeckel, A synthetic antithrombin III binding pentasaccharide is now a drug! What comes next? *Angew. Chem. Int. Ed.* **43**, 3118–3133 (2004).
12. Y. Xu, C. Cai, K. Chandarajoti, P.-H. Hsieh, L. Li, T. Q. Pham, E. M. Sparkenbaugh, J. Sheng, N. S. Key, R. Pawlinski, E. N. Harris, R. J. Linhardt, J. Liu, Homogeneous low-molecular-weight heparins with reversible anticoagulant activity. *Nat. Chem. Biol.* **10**, 248–250 (2014).
13. J. Liu, R. J. Linhardt Chemoenzymatic synthesis of heparan sulfate and heparin. *Nat. Prod. Rep.* **31**, 1676–1685 (2014).
14. J. Chen, F. Y. Avci, E. M. Muñoz, L. M. McDowell, M. Chen, L. C. Pedersen, L. Zhang, R. J. Linhardt, J. Liu, Enzymatically redesigning of biologically active heparan sulfate. *J. Biol. Chem.* **280**, 42817–42825 (2005).
15. Z. Zhang, S. A. McCallum, J. Xie, L. Nieto, F. Corzana, J. Jiménez-Barbero, M. Chen, J. Liu, R. J. Linhardt, Solution structure of chemoenzymatically synthesized heparin and its precursors. *J. Am. Chem. Soc.* **130**, 12998–13007 (2008).
16. Y. Xu, S. Masuko, M. Takieddin, H. Xu, R. Liu, J. Jing, S. A. Mousa, R. J. Linhardt, J. Liu, Chemoenzymatic synthesis of homogeneous ultralow molecular weight heparins. *Science* **334**, 498–501 (2011).
17. Y. Xu, A. F. Moon, S. Xu, J. M. Krahn, J. Liu, L. C. Pedersen, Structure based substrate specificity analysis of heparan sulfate 6-*O*-sulfotrasnferases. *ACS Chem. Biol.* **12**, 73–82 (2016).
18. B. Kuberan, M. Z. Lech, D. L. Beeler, Z. L. Wu, R. D. Rosenberg, Enzymatic synthesis of antithrombin III-binding heparan sulfate pentasaccharide. *Nat. Biotechnol.* **21**, 1343–1346 (2003).
19. L. Li, F. Zhang, J. Zaia, R. J. Linhardt, Top-down approach for the direct characterization of low molecular weight heparins using LC-FT-MS. *Anal. Chem.* **84**, 8822–8829 (2012).
20. I. Singh, A. Smith, B. Vanzieleghem, D. Collen, K. Burnand, J.-M. Saint-Remy, M. Jacquemin, Antithrombotic effects of controlled inhibition of factor VIII with a partially inhibitory human monoclonal antibody in a murine vena cava thrombosis model. *Blood* **99**, 3235–3240 (2002).
21. S. P. Grover, C. E. Evans, A. S. Patel, B. Modarai, P. Saha, A. Smith, Assessment of venous thrombosis in animal models. *Arterioscler. Thromb. Vasc. Biol.* **36**, 245–252 (2016).
22. C. Pászty, C. M. Brion, E. Manci, H. E. Witkowska, M. E. Stevens, N. Mohandas, E. M. Rubin, Transgenic knockout mice with exclusively human sickle hemoglobin and sickle cell disease. *Science* **278**, 876–878 (1997).
23. P. Chantrathammachart, N. Mackman, E. Sparkenbaugh, J.-G. Wang, L. V. Parise, D. Kirchhofer, N. S. Key, R. Pawlinski, Tissue factor promotes activation of coagulation and inflammation in a mouse model of sickle cell disease. *Blood* **120**, 636–646 (2012).
24. E. M. Sparkenbaugh, P. Chantrathammachart, J. Mickelson, J. van Ryn, R. P. Hebbel, D. M. Monroe, N. Mackman, N. S. Key, R. Pawlinski, Differential contribution of FXa and thrombin to vascular inflammation in a mouse model of sickle cell disease. *Blood* **123**, 1747–1756 (2014).
25. E. Sparkenbaugh, R. Pawlinski, Interplay between coagulation and vascular inflammation in sickle cell disease. *Br. J. Haematol.* **162**, 3–14 (2013).
26. G. J. Kato, M. H. Steinberg, M. T. Gladwin, Intravascular hemolysis and the pathophysiology of sickle cell disease. *J. Clin. Invest.* **127**, 750–760 (2017).
27. P. I. Arumugam, E. S. Mullins, S. K. Shanmukhappa, B. P. Monia, A. Loberg, M. A. Shaw, T. Rizvi, J. Wansapura, J. L. Degen, P. Malik, Genetic diminution of circulating prothrombin ameliorates multiorgan pathologies in sickle cell disease mice. *Blood* **126**, 1844–1855 (2015).
28. K. A. Nath, R. P. Hebbel, Sickle cell disease: Renal manifestations and mechanisms. *Nat. Rev. Nephrol.* **11**, 161–171 (2015).
29. N. Bank, H. S. Aynedjian, J.-H. Qiu, S. Y. Osei, R. S. Ahima, M. E. Fabry, R. L. Nagel, Renal nitric oxide synthases in transgenic sickle cell mice. *Kidney Int.* **50**, 184–189 (1996).
30. J. Hirsh, M. O. O'Donnell, J. W. Eikelboom, Beyond unfractionated heparin and warfarin: Current and future advances. *Circulation* **116**, 552–560 (2007).
31. Agency for Toxic Substances and Disease Registry, Toxicologal profile for nitrophenols; www.atsdr.cdc.gov/toxprofiles/tp.asp?id=880&tid=172.
32. I. Mahé, J. Chidac, H. Helfer, S. Nobel, Factors influencing adherence to clinical guidelines in the management of cancer-associated thrombosis. *J. Thromb. Haemost.* **14**, 2017–2113 (2016).
33. B. P. McDonnell, K. Glennon, A. McTiernan, H. D. O'Connor, C. Kirkham, B. Kevane, J. C. Donnelly, F. Ni Áinle, Adjustment of therapeutic LMWH to achieve specific target anti-FXa activity does not affect outcomes in pregnant patients with venous thromboembolism. *J. Thromb. Thrombolysis* **43**, 105–111 (2017).
34. P. Sinaÿ, J.-C. Jacquinet, M. Petitou, P. Duchaussoy, I. Lederman, J. Choay, G. Torri, Total synthesis of a heparin pentasaccharide fragment having high affinity for antithrombin III. *Carbohydr. Res.* **132**, C5–C9 (1984).
35. C. A. A. van Boeckel, T. Beetz, J. N. Vos, A. J. M. de Jong, S. F. Van Aelst, R. H. van den Bosch, J. M. R. Mertens, F. A. van der Vlugt, Synthesis of a pentasaccharide corresponding to the antithrombin III binding fragment of heparin. *J. Carbohydr. Chem.* **4**, 293–321 (1985).
36. P.-A. Driguez, P. Potier, P. Trouileux, Synthetic oligosaccharides as active pharmaceutical ingredients: Lessons learned from the full synthesis of one heparin derivative on a large scale. *Nat. Prod. Rep.* **31**, 980–989 (2014).
37. W. Jeske, E. Litinas, H. Khan, D. Hoppensteadt, J. Fareed, A comparison of the pharmacodynamic behavior of branded and biosimilar enoxaparin in primates. *Clin. Appl. Thromb./Hemostasis* **18**, 294–298 (2012).

38. E. Young, V. Douros, T. J. Podor, S. G. Shaughnessy, J. I. Weitz, Localization of heparin and low-molecular-weight heparin in the rat kidney. *Thromb. Haemost.* **91**, 927–934 (2004).
39. M. A. Smythe, J. Priziola, P. P. Dobesh, D. Wirth, A. Cuker, A. K. Wittkowsky, Guidance for the practical management of the heparin anticoagulants in the treatment of venous thromboembolism. *J. Thromb. Thrombolysis* **41**, 165–186 (2016).
40. M. T. Kalathottukaren, L. Abraham, P. R. Kapopara, B. F. L. Lai, R. A. Shenoi, F. I. Rosell, E. M. Conway, E. L. G. Pryzdial, J. H. Morrissey, C. A. Haynes, J. N. Kizhakkedathu, Alteration of blood clotting and lung damage by protamine are avoided using the heparin and polyphosphate inhibitor UHRA. *Blood* **129**, 1368–1379 (2017).
41. R. A. Shenoi, M. T. Kalathottukaren, R. J. Travers, B. F. L. Lai, A. L. Creagh, D. Lange, K. Yu, M. Weinhart, B. H. Chew, C. Du, D. E. Brooks, C. J. Carter, J. H. Morrissey, C. A. Haynes, J. N. Kizhakkedathu, Affinity-based design of a synthetic universal reversal agent for heparin anticoagulants. *Sci. Tansl. Med.* **6**, 260ra150 (2014).
42. G. Lu, F. R. DeGuzman, S. J. Hollenbach, M. J. Karbarz, K. Abe, G. Lee, P. Luan, A. Hutchaleelaha, M. Inagaki, P. B. Conley, D. R. Phillips, U. Sinha, A specific antidote for reversal of anticoagulation by direct and indirect inhibitors of coagulation factor Xa. *Nat. Med.* **19**, 446–451 (2013).
43. D. M. Siegal, J. T. Curnutte, S. J. Connolly, G. Lu, P. B. Conley, B. L. Wiens, V. S. Mathur, J. Castillo, M. D. Bronson, J. M. Leeds, F. A. Mar, A. Gold, M. A. Crowther, Andexanet alfa for the reversal of factor Xa inhibitor activity. *N. Engl. J. Med.* **373**, 2413–2424 (2015).
44. S. J. Connolly, T. J. Milling Jr., J. W. Eikelboom, C. M. Gibson, J. T. Curnutte, A. Gold, M. D. Bronson, G. Lu, P. B. Conley, P. Verhamme, J. Schmidt, S. Middeldorp, A. T. Cohen, J. Beyer-Westendorf, P. Albaladejo, J. Lopez-Sendon, S. Goodman, J. Leeds, B. L. Wiens, D. M. Siegal, E. Zotova, B. Meeks, J. Nakamya, W. T. Lim, M. Crowther; ANNEXA-4 Investigators, Andexanet alfa for acute major bleeding associated with factor Xa inhibitors. *N. Engl. J. Med.* **375**, 1131–1141 (2016).
45. P.-H. Hsieh, Y. Xu, D. A. Keire, J. Liu, Chemoenzymatic synthesis and structural characterization of 2-*O*-sulfated glucuronic acid containing heparan sulfate hexasaccharides. *Glycobiology* **24**, 681–692 (2014).
46. L. Zhang, D. L. Beeler, R. Lawrence, M. Lech, J. Liu, J. C. Davis, Z. Shriver, R. Sasisekharan, R. D. Rosenberg, 6-*O*-sulfotransferase-1 represents a critical enzyme in the anticoagulant heparan sulfate biosynthetic pathway. *J. Biol. Chem.* **276**, 42311–42321 (2001).
47. M. B. Duncan, J. Chen, J. P. Krise, J. Liu, The biosynthesis of anticoagulant heparan sulfate by the heparan sulphate 3-*O*-sulfotransferase isoform 5. *Biochim. Biophys. Acta* **1671**, 34–43 (2004).
48. Y. Xu, E. Pempe, J. Liu, Chemoenzymatic synthesis of heparin oligosaccharides with both anti-factor Xa and anti-factor IIa activities. *J. Biol. Chem.* **287**, 29054–29061 (2012).
49. M. Sundaram, Y. Qi, Z. Shriver, D. Liu, G. Zhao, G. Venkataraman, R. Langer, R. Sasisekharan, Rational design of low-molecular weight heparins with improved in vivo activity. *Proc. Natl. Acad. Sci. U.S.A.* **100**, 651–656 (2003).
50. D. A. Ferenbach, N. C. Nkejabega, J. McKay, A. K. Choudhary, M. A. Vernon, M. F. Beesley, S. Clay, B. C. Conway, L. P. Marson, D. C. Kluth, J. Hughes, The induction of macrophage hemeoxygenase-1 is protective during acute kidney injury in aging mice. *Kidney Int.* **79**, 966–976 (2011).
51. S. C. Gad, *Drug Safety Evaluation* (John Wiley and Sons Inc., 2002), pp. 130–175.
52. R. Liu, Y. Xu, M. Chen, M. Weïwer, X. Zhou, A. S. Bridges, P. L. DeAngelis, Q. Zhang, R. J. Linhardt, J. Liu, Chemoenzymatic design of heparan sulfate oligosaccharides. *J. Biol. Chem.* **285**, 34240–34249 (2010).
53. D. Xu, A. F. Moon, D. Song, L. C. Pedersen, J. Liu, Engineering sulfotransferases to modify heparan sulfate. *Nat. Chem. Biol.* **4**, 200–202 (2008).
54. J. Liu, Z. Shriver, P. Blaiklock, K. Yoshida, R. Sasisekharan, R. D. Rosenberg, Heparan sulfate D-glucosaminyl 3-*O*-sulfotransferase-3A sulfates *N*-unsubstituted glucosamine residues. *J. Biol. Chem.* **274**, 38155–38162 (1999).
55. M. Chen, A. Bridges, J. Liu, Determination of the substrate specificities of *N*-acetyl-D-glucosaminyl transferase. *Biochemistry* **45**, 12358–12365 (2006).
56. G. Zhao, W. Guan, L. Cai, P. G. Wang, Enzymatic route to preparative-scale synthesis of UDP-GlcNAc/GalNAc, their analogues and GDP-fucose. *Nat. Protoc.* **5**, 636–646 (2010).
57. X. Zhou, K. Chandarajoti, T. Q. Pham, R. Liu, J. Liu, Expression of heparan sulfate sulfotransferases in *Kluyveromyces lactis* and preparation of 3′-phosphoadenosine-5′-phosphosulfate. *Glycobiology* **21**, 771–780 (2011).

Funding: This work was supported by grants from the NIH (GM102137, HL62244, HL117659, and HL094463), Eshelman Innovation Institute, and North Carolina Translational and Clinical Sciences Institute. Both J.L. and R.J.L. laboratories are subcontractors for Glycan Therapeutics LLC for NIH Small Business Innovation Research contract HHSN261201500019C. J.L. and R.J.L. laboratories are also supported by a grant from the U.S. FDA (U19FD004994). In addition, J.L. laboratory was supported by NIH grants U01HL117659 (to K. Ataga), R01GM072667 (to X. Huang), R01HL056819 (to E. Chaikov), U01 GM116262 (to L. Hsieh-Wilson), and 1R01 HL 130864 (to E. Harris) and a grant from Vesta Therapeutics Inc. (to L. Reid). R.J.L. laboratory is also supported by NSF grants R01HL125371 (to E. Schmidt), R01NS088496 (to Y. Yamaguchi), 3R01GM049975 (to L. Kiessling), and 1362234 (to L. Schadler). R.P. laboratory was supported by NIH grant U01HL117659. N.S.K. laboratory was supported by the following NIH grants: U01 HL117659 (to K. Ataga), U01 HL122894 (to T. Gernsheimer), R01 AI126542 (to J. Baker), T32 HL007149 (to N.S.K.), and UL1-TR00111 (to J. Buse). **Author contributions:** Y.X. and J.L. developed and completed the synthetic scheme to prepare 12-mers. K.C., E.M.S., B.C., and R.P. evaluated the anticoagulant efficacy of 12-mer-1 in mice studies. X.Z. and R.J.L. conducted and designed the experiments to prove the structures of 12-mers. V.P. and W.D. improved the enzyme expression and cofactor synthesis. D.M.H. and J.F. conducted and designed the experiment to determine the pharmacodynamic properties of 12-mer-1. S.D. and D.S.-S. designed and supervised the toxicity study of 12-mer-1 in rat. N.S.K. contributed to the design of synthetic heparin for clinical applications. J.L., R.P., and R.J.L. designed the project and wrote the manuscript. All authors participated in writing the manuscript. **Competing interests:** Y.X. and J.L. are founders of Glycan Therapeutics LLC, and V.P. is an employee of Glycan Therapeutics LLC. J.L., R.J.L., and Y.X. are inventors of a pending patent application US2016/0122446A1, which is owned by UNC, Rensselaer Polytechnic Institute, and University of Nebraska at Lincoln. The patent covers similar structures, but not the same ones described in the present study, of synthetic LMWH. Glycan Therapeutics LLC has licensed the patent. All other authors declare that they have no competing interests.

Submitted 5 May 2017
Accepted 7 August 2017
Published 6 September 2017
10.1126/scitranslmed.aan5954

Citation: Y. Xu, K. Chandarajoti, X. Zhang, V. Pagadala, W. Dou, D. M. Hoppensteadt, E. M. Sparkenbaugh, B. Cooley, S. Daily, N. S. Key, D. Severynse-Stevens, J. Fareed, R. J. Linhardt, R. Pawlinski, J. Liu, Synthetic oligosaccharides can replace animal-sourced low–molecular weight heparins. *Sci. Transl. Med.* **9**, eaan5954 (2017).

Science Translational Medicine

Synthetic oligosaccharides can replace animal-sourced low–molecular weight heparins

Yongmei Xu, Kasemsiri Chandarajoti, Xing Zhang, Vijayakanth Pagadala, Wenfang Dou, Debra Moorman Hoppensteadt, Erica M. Sparkenbaugh, Brian Cooley, Sharon Daily, Nigel S. Key, Diana Severynse-Stevens, Jawed Fareed, Robert J. Linhardt, Rafal Pawlinski and Jian Liu

Sci Transl Med **9**, eaan5954.
DOI: 10.1126/scitranslmed.aan5954

A reliable animal-free heparin drug

Full-sized and low–molecular weight heparins are widely used to treat a variety of clotting disorders. Although low–molecular weight heparins are safer and more convenient to use than full-size heparin, they are still animal-derived products that present a risk of contamination and supply chain interruptions and are limited with respect to standardization and reversibility of anticoagulation. A method developed by Xu *et al.* offers a potential alternative to animal-sourced heparins in the form of a chemical synthesis process that can be scaled up to produce heparin dodecasaccharides with reversible activity in adequate quantities for potential therapeutic use.